Reconstruction of the uncompensated electron momentum density distribution by the maximum entropy method

1999 J. Phys.: Condens. Matter 11 8049

(http://iopscience.iop.org/0953-8984/11/41/308)

J. Phys.: Condens. Matter **11** (1999) 8049–8060. Printed in the UK PII: S0953-8984(99)01817-2

Reconstruction of the uncompensated electron momentum density distribution by the maximum entropy method

L Dobrzynski†‡ and E Zukowski†

† Institute of Physics, University of Bialystok, Lipowa 41, 15-424 Bialystok, Poland
‡ Laboratoire de Minéralogie-Cristallographie, Université de Paris VI, 4 place Jussieu, 75252 Paris Cedex 05, France and The Soltan Institute for Nuclear Studies, 05-400 Otwock-Swierk, Poland

E-mail: ludwik@fuw.edu.pl (L Dobrzynski)

Received 12 February 1999, in final form 16 July 1999

Abstract. The application of the maximum entropy method (MEM) to the reconstruction of the three-dimensional electron momentum density for electrons with uncompensated spins is described. The case of iron, for which the largest collection of experimental data is available, is presented in detail. The analysis of the distributions in Fe_3Si and Cu_2MnAl alloys is carried out based on measurements of the magnetic Compton profiles along only three high-symmetry crystallographic directions. It is shown that the general density distributions in Fe and Fe_3Si are very much alike, while the data for Cu_2MnAl can be interpreted with a single strictly positive distribution. It is postulated that the crater-like structure of the magnetic Compton profiles may be due to both conduction and d-band polarizations. In such a case one could reconcile the results of the neutron and Compton experiments.

1. Elements of the maximum entropy method

In accordance with the well known approach (Jaynes 1983), the information entropy of the distribution $f(x)$ which fulfils the requirements of positivity and additivity is given by

$$S = -\sum f(x)\ln[f(x)] \tag{1}$$

where the summation runs over all values of x. If the space of x is divided into N pixels numerated by an index i, equation (1) can be rewritten as

$$S = -\sum f_i \ln(f_i) \tag{2}$$

where f_i denotes the value of $f(x)$ in the ith pixel.

Let us now assume that one is having M measurements which are expected to be described by a function $G\{j; f(x)\}$, i.e. every data point d_j ($j = 1, \ldots, M$) should be described as

$$d_j = G\{j; f(x)\} + e_j = G_j + e_j \tag{3}$$

where e_j denotes a noise, usually assumed to be Gaussian. Then the goodness of our choice of G-function is quantified through the likelihood function

$$P_L = A\exp(-\chi^2/2) \tag{4}$$

where A denotes a normalization constant and

$$\chi^2 = \sum \left(\frac{d_j - G_j}{e_j}\right)^2 \tag{5}$$

0953-8984/99/418049+12$30.00

is the usual misfit function to be minimized in order to obtain the maximum value of the likelihood function. Obviously, G_j in equations (3) and (5) is the shortened abbreviation of the function $G\{j; f(x)\}$.

Actually, maximization of the likelihood function may not be the only goal of the experimentalists who want to search for the best function $f(x)$, which describes the data. In accordance with the idea of the maximum entropy method (MEM), the function $f(x)$ which is compatible with the experimental data and is making least use of the unavailable information is the one which maximizes information entropy

$$S = -\sum\{f_j \ln(f_j/m_j) - [f_j - m_j]\} \tag{6}$$

where $m_j = m(x_j)$ is the default function or the distribution known prior to carrying out the experiment, or any modelled distribution which may be expected on some physical grounds. If nothing is known about the searched for distribution $f(x)$, a uniform distribution $m(x) = \text{const}$ is used as the prior. Using the undetermined Lagrange multipliers method one is maximizing finally the following Lagrangian:

$$L = S - \lambda[(\chi^2 - \chi^2_{aim})/2] \tag{7}$$

where λ is a positive Lagrange multiplier, which should be chosen in such a way that the maximization of the Lagrangian (7) would result in $\chi^2 = \chi^2_{aim}$. It is customary to set the latter to the number M of the measured points.

Illustrating examples of the use of the maximum entropy method can be found in various conference proceedings (edited by Smith and Grandy (1985), Skilling (1988, 1989), Erickson and Smith (1988) and Mohammad-Djafari and Demoments (1993)). The basic routines are also commercially available (Gull and Skilling 1989). In the case of reconstruction of the charge density distribution one can use the program package MEED (Sakata and Sato 1990, Sakata *et al* 1993) distributed free of charge. After a small modification this same package can be used for internal magnetization distribution (see e.g. Dobrzynski *et al* 1996). In both cases, however, one should be careful with conclusions because the MEM can occasionally produce spurious details in the searched for distributions (see e.g. the critique by Jauch (1994)).

We shall focus our attention on the application of the maximum entropy method to the reconstruction of the momentum density for electrons with uncompensated spins from the set of experimentally measured so-called magnetic Compton profiles. The essential MEM ideas are the same as used in Dobrzynski *et al* (1996). Because the searched for distribution can be negative, one is composing it from two strictly positive distributions $f_+(x)$ and $f_-(x)$, following e.g. Papoular and Gillon (1990). These distributions, however, should not be interpreted as describing the 'up' and 'down' spin electrons. The total entropy is now $S = S_+ + S_-$, where

$$S_\sigma = -\sum p_\sigma \ln(p_\sigma/m_\sigma) \tag{8}$$

with $\sigma = +, -$ (summation runs over all pixels or rather voxels) and

$$p_\sigma = f_\sigma \left(\sum (f_+ + f_-)\right)^{-1}. \tag{9}$$

The maximization of the Lagrangian is carried out with respect to both p_+ and p_- functions. As a result one obtains $2N_{pix}$ strongly nonlinear equations, where N_{pix} denotes the number of voxels in which the densities are to be determined.

In order to normalize f_σ functions, a parameter α defined as follows will be used:

$$\mu_+ = (1+\alpha)\mu_{spin,tot} = \sum f_+ \tag{10}$$

and

$$\mu_- = -\alpha\mu_{spin,tot} = -\sum f_- \tag{11}$$

where $\mu_{spin,tot}$ denotes the total spin magnetic moment that must be preserved throughout the calculations (see section 4). Let us note that the search of a strictly positive distribution means setting α at zero and using only one of the two components of the sums in equations (8) and (9).

2. Electron momentum distributions

Electron momentum density distributions are measured in the x- or γ-ray scattering experiments. The shape of the Compton line, the so-called Compton profile, is

$$J(p_z) = \int n(p_x, p_y, p_z)\,\mathrm{d}p_x\,\mathrm{d}p_y \tag{12}$$

where $n(\boldsymbol{p})$ is the three-dimensional electron momentum density distribution and the z-axis is determined by the geometry of the experiment. The problems encountered in the reconstructions of the $n(\boldsymbol{p})$ from the sets of $J(p_z)$ measured along various directions were described by Dobrzynski and Holas (1996).

In the so-called magnetic Compton scattering one measures the difference between the 'up' and 'down' Compton profiles, i.e.

$$J_{mag}(p_z) = \int [n_+(\boldsymbol{p}) - n_-(\boldsymbol{p})]\,\mathrm{d}p_x\mathrm{d}p_y. \tag{13}$$

The integral of $J_{mag}(p_z)$ over p_z must be equal to $\mu_{spin,tot}$. The difference of the 'up' and 'down' densities may be positive and negative, so the reconstruction of this difference function requires calculations similar to the ones carried out in order to reconstruct a magnetization distribution (see e.g. Papoular and Gillon 1990, Dobrzynski 1995). Maximization of the entropies with respect to both 'up' and 'down', densities (such a procedure is also called two-channel MEM) requires prior knowledge of the parameter α or some features of the function to be reconstructed. For example, one can seek solutions that are strictly positive at large momenta and decay to almost zero at a certain momentum value. One can also be guided by the anisotropy of the distribution or the momentum value below which negative solutions are expected. As can be seen, if one is completely ignorant regarding the searched for distribution, the results obtained can be physical only when a sufficient number of high-quality experimental data is accumulated.

3. Technical details of the reconstructions of the electron momentum densities

The problem that arises immediately when we start to work with the MEM algorithm is the fitness of the grid that should be used for the reconstruction. A typical range of electron momenta contributing to the Compton profiles is from about -12 au to +12 au (where 1 atomic unit, 1 au $= 1.99 \times 10^{-24}$ kg m s^{-1}; this value follows from the adopted convention in which $\hbar = m = e = 1, c = 137$), so the space to be covered by the grid is very large. Typical measurements are carried out with the momentum step of 0.1 au, which means that in order to reconstruct the density with similar resolution one needs to use a grid of $241^3 = 1.4 \times 10^7$ voxels! Required symmetry of the distribution will reduce this number by 48 in the case of cubic symmetry. However, even having to calculate the densities in these 3×10^5 voxels which are left signifies that one has a difficult computational problem.

Let us now consider a relationship between the density n_i in the ith voxel and the available experimental information. Let the Compton profiles be measured at N_{max} points for every direction $j = 1, \ldots, N_{dir}$. In other words, the experiment delivers the values $J_j(p_i)$, where

$i = 1, \ldots, N_{max}$. The surface integrals (13) can be represented as sums, so one expects that

$$J_j(p_i) = \sum_{j=1}^{N_{dir}} \sum_{i=1}^{N_{\max}} \sum_{k=1}^{N_{pix}} a(j, i, k) n_k + e_{ji} \tag{14}$$

where the subscript *mag* was omitted for simplicity. The coefficients $a(j, i, k)$ are not trivial, so they should be calculated only once at the beginning of the reconstruction. This saves computing time but costs computer memory because the matrix $a(j, i, k)$ easily occupies hundreds of megabytes of memory. A computer program written by us is capable to calculate the coefficients $a(j, i, k)$ for cubic, hexagonal and tetragonal structures. The integrations can be carried out over respective polygons or over a sphere. It was shown that the latter leads as a rule to lower accuracy of the results and therefore is not practical. The general calculation scheme in solving MEM equations is the same as used in the MEED package.

4. Reconstruction of the three-dimensional momentum density for the uncompensated spins in iron

There are no simple methods which permit us to carry out a reliable reconstruction without previous knowledge or expectations of some important details in the density distribution that one is going to retrieve from the experimental data. Normally the total magnetic moment is known. However, because the Compton scattering at high energies senses the spin moment only, even this information may sometimes be insufficient. Happily, in the case of iron, the orbital moment is known fairly well, so at least the value of the magnetic moment that contributes to the magnetic Compton profile is known. In the following, the results obtained for iron by Tanaka *et al* (1993) will be analysed. As mentioned previously, the reconstruction of interest involves positive and negative densities. Normalization of their difference is known only, so the multitude of resultant distributions can be obtained (Dobrzynski and Holas 1995).

First the reconstruction within a cube of side 10 au, and voxel size (0.1 au) $\times$ (0.1 au) $\times$ (0.1 au) was carried out. The cube contained positive momenta (including zero) only. Using the cubic symmetry constraints the number of independent voxels in which the densities were calculated was 176 851. The number of maximum entropy equations that one has to solve was thus 353 702. The experimental results within the range of up to 10 au for the high-symmetry directions $\langle 100\rangle$, $\langle 110\rangle$, $\langle 111\rangle$ and $\langle 112\rangle$ were used at the beginning. A series of calculations have been carried out for a variety of values of the parameter α. In every case, the program converged and was delivering reconstruction which described the experiment sufficiently well in the sense of the χ^2-test. We show two such reconstructions in figures 1 and 2, the former carried out for $\alpha = 1.0$, the latter for $\alpha = 0.5$. In contrast to the procedure used by Dobrzynski and Holas (1995), a nonuniform prior was used. It follows from the paper by Tanaka *et al* (1993) that the prior should be predominantly negative in the momentum region of up to 1.4 au, and predominantly positive above this value. The prior momentum densities in both parts of the space were kept uniform. Three results should be mentioned:

- while the positive part of the reconstructed distribution does not seem to be too sensitive to the initial assumptions, the value of α is quite essential for seeing the details in the negative part of the density distribution,
- if one integrates separately the positive and negative parts of the resultant density, $n_+ - n_-$, the sum of which gives the spin magnetic moment, one clearly sees that the negative moment corresponds to a much lower value of α than initially assumed. While such a decrease can be expected on general grounds, the scale of this effect turns out to be, however, unexpectedly large. For the two cases presented in figures 1 and 2, the values

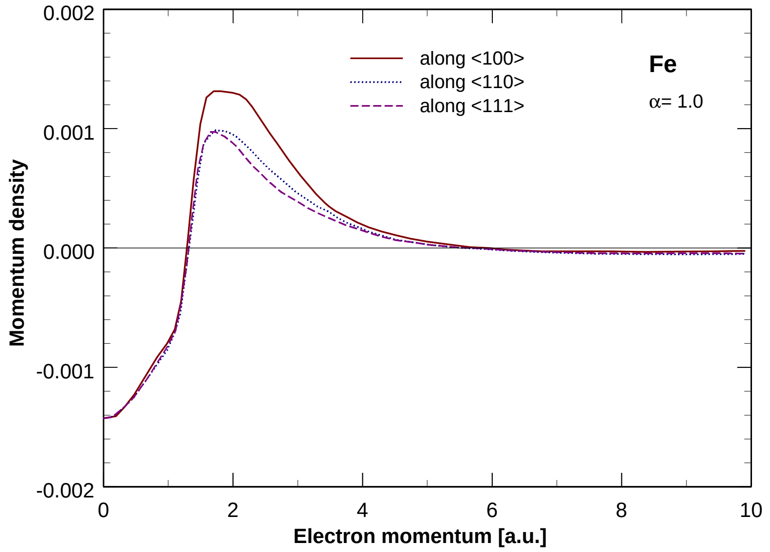

Figure 1. Reconstruction of the momentum density distribution for uncompensated spins in iron along three high-symmetry directions. The case of $\alpha = 1.0$ in the nonuniform prior. Four high-symmetry directions used in the reconstruction.

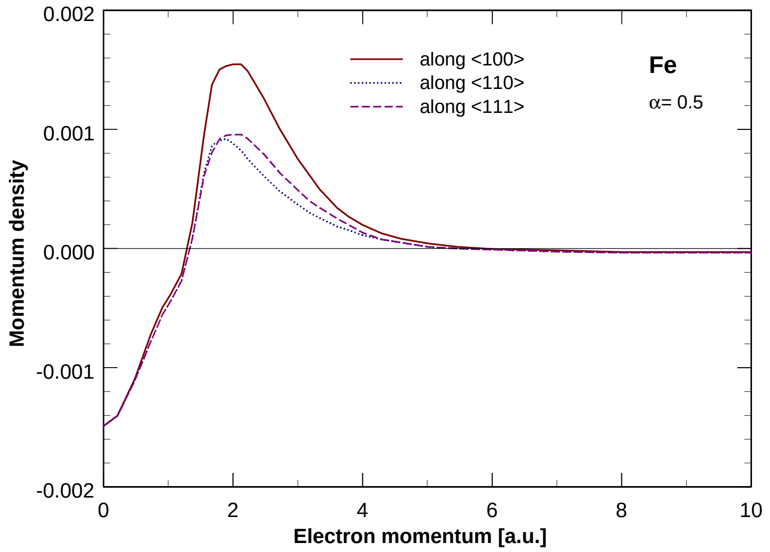

Figure 2. Same as figure 1 but for $\alpha = 0.5$.

of positive and negative moments (in arbitrary but the same units following from the normalization of the experimental Compton profile and the voxel size; in order to obtain the moments in Bohr magnetons one has to multiply the quoted values by about 10) are 0.210 and -0.016 for $\alpha = 1$ and 0.207 and -0.011 for $\alpha = 0.5$. These values correspond to α values equal roughly to 0.08 and 0.06, respectively. It is clear that neither the shape of the negative part nor the absolute value of the negative moment can be well determined unless further assumptions are made,

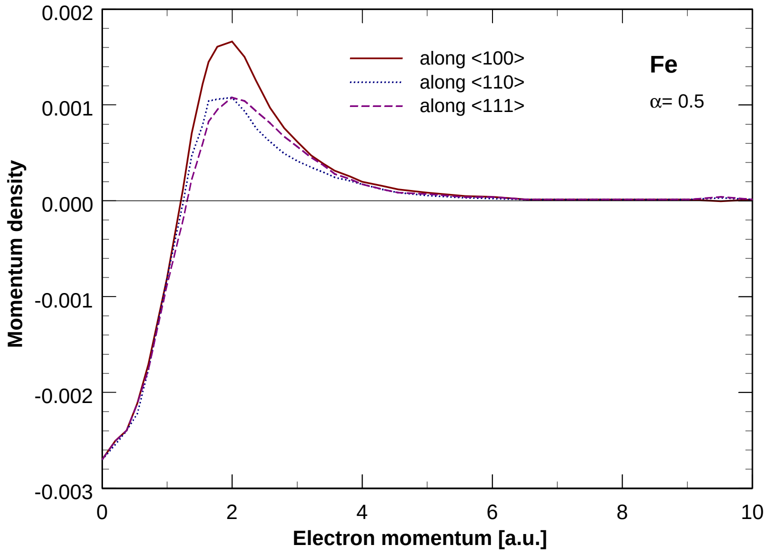

Figure 3. Results of the reconstruction based on all 14 directions measured; see text for details.

- for larger α values, quite a substantial part of the negative density appears at high momenta which is not physical. Therefore one obtains at least an indication that the reconstruction carried out, say, for $\alpha = 0.5$ is more likely than the other one. In fact, starting from a completely uniform prior within a cube of size 10 au, even for this latter value of α one obtains the negative net density at larger momenta. One can obtain some improvement (more negative density at low momenta) if the uniform prior is limited to a smaller volume; nevertheless the negative densities at larger momenta are preferred. These observations indicate that the information content in the results of the magnetic Compton profiles for the four aforementioned crystallographic directions is insufficient for reliable reconstruction of the negative part of the density unless one adds an extra information. For example, if one knows that the negative density cannot appear above momentum of, say, 1.4 au, the immediate result is that one should use a non-uniform prior and α less than approximately 0.5.

In the next step the experimental results for five off-symmetry directions, $\langle 013\rangle$, $\langle 023\rangle$, $\langle 012\rangle$, $\langle 133\rangle$ and $\langle 223\rangle$, were also included. This resulted immediately in the cancellation of negative densities at high momenta. The positive part was, as expected, not seriously altered. This time, however, the negative densities at low momenta appeared to have very inhomogeneous, almost conical distribution. It is apparent that one should use all experimental information available, results for all 14 directions measured. In order to reduce increased computational effort, each side (of the 10 au length) was divided this time into 50 pixels only, and every second experimental point only (distant from each other by 0.2 au) from the range up to 7.1 au was taken into account. The reconstructed density, which is shown in figure 3, leads to magnetic Compton profiles which fit excellently to the experimental data. One notes that the total negative moment obtained is apparently larger than previously obtained and the negative valley is deeper. One could of course now study the influence of the initial value of α on the depth and shape of this valley. What we, however, found more important was to see whether one cannot obtain a more uniform distribution of the density within the valley. With this idea in mind we have chosen a prior in which the positive part was as in the result just described, while a cylindrical well was used as a prior in the negative part. Of course, the negative densities

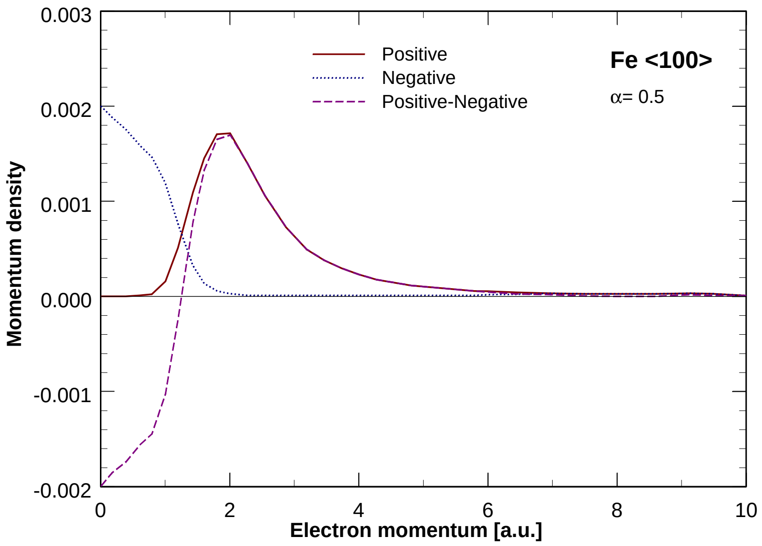

Figure 4. Positive, negative and resultant densities as directly obtained in the course of calculations for the ⟨100⟩ direction (the resultant density is the same as in figure 3).

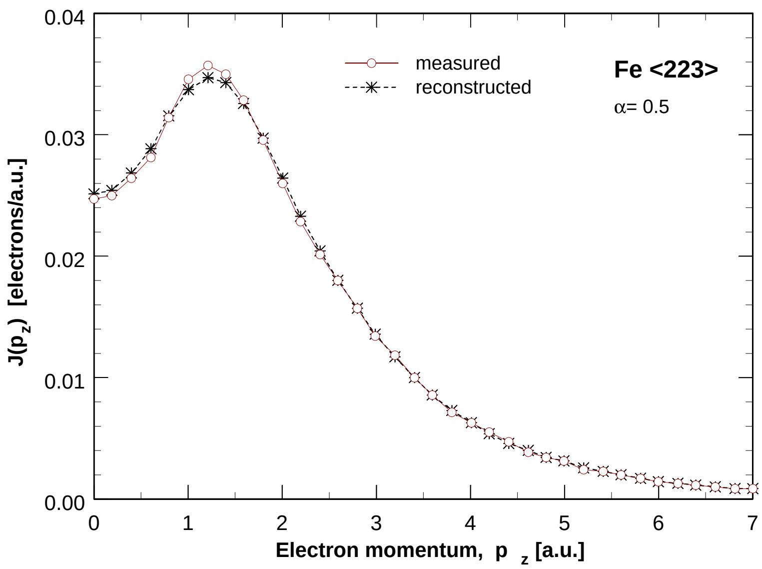

Figure 5. The comparison of measured and reconstructed magnetic Compton profiles for the ⟨223⟩ direction, for which the reconstruction was the worst one.

were integrating out to the appropriate value of the magnetic moment. The final result was not fundamentally different from the one shown in figure 3. It is worth noticing that although in all priors non-analytical distributions were introduced, the reconstructed densities are behaving properly, and so both positive and negative partial densities are as well, see figure 4. How well the reconstructed density fits the experiment may be illustrated by making a comparison of the measured and reconstructed magnetic Compton profiles. Such a comparison for the ⟨223⟩ direction for which agreement is the worst, χ^2 on the level of 1.6, is displayed in figure 5.

For most of the directions the χ^2 parameter is less than 1.0, which means that the reconstructed points are hardly distinguishable from the measured ones.

In conclusion, we can say that the measured 14 directions for iron may be sufficient for a reliable three-dimensional reconstruction providing extra information is included in the calculations. This information may be, for example, the value of the total negative moment, which should appear at low momenta. If this moment was uniquely due to conduction electrons then, based on the neutron results of Shull and Yamada (1962), one could expect the value of $-0.16\ \mu_B$/atom, while the recent theoretical estimate (Eriksson *et al* 1992) gives $-0.07\ \mu_B$/atom. Within the normalization of the magnetic Compton profiles used here these values are: -0.018 and -0.007, correspondingly. Personally, we believe more in the latter value (see Dobrzynski 1974, van Laar *et al* 1980, Dobrzynski *et al* 1996).

Leaving the value of negative moment aside, one can raise an important question on what such an integrated negative moment really represents. We note that the depth of the valley seen e.g. in figure 4 agrees quite well with the theoretically obtained one, which was shown in the paper by Tanaka *et al* (1993). If the integrated negative density were ascribed solely to the diffuse part of the magnetic moment, this would imply that the d-type magnetic density would be practically zero at low momenta. On the other hand, if the d-part of the density continued to grow below, say, 1.5 au, a relatively large negative moment would be needed in order to compensate for such growth of the positive moment. Therefore we believe that the d-part itself of the momentum density for spin-uncompensated electrons must have some crater-like structure around zero momentum. This in fact may be quite natural in light of the exchange polarization among d electrons, which leads to the dependence of the wavefunction on the spin of the electron. This effect, which is generally responsible for the appearance of hyperfine fields on nuclei, leads to the relative contraction of the d wavefunction of the electron with spin up with respect to the wavefunction for the spin-down electron. At large distances from the atomic centres and, correspondingly, at low momenta, one can thus expect even negative 3d-type densities. It is also possible that the hybridization of d and (s, p) electrons in the low momentum range does not permit us to make any sensible distinction between these electrons.

It may be interesting to note that the 3d-part of the momentum density shows clearly e_g-type symmetry, known already from the neutron measurements but seen here with sensitivity enhanced with respect to the neutron case.

5. Reconstruction of the three-dimensional momentum density for the uncompensated spins in Fe_3Si

The magnetization distribution in Fe_3Si was analysed by Dobrzynski (1995) who showed that any homogenous negative magnetic moment is hardly visible in this alloy. Very recent magnetic Compton scattering data (Zukowski *et al* 2000) brought, however, magnetic Compton profiles strikingly similar to the ones for iron. Indeed, the reconstruction based on the only available data for three high-symmetry directions shows a characteristic negative valley as in the case of iron. Again, clear e_g-type symmetry of the magnetic moment is seen. However, because in this case the measurements have been carried out along three high-symmetry directions only, one should be particularly careful with choosing the appropriate prior. The distributions along $\langle 100\rangle$ directions obtained for various values of the parameter α are shown in figure 6. Because of the neutron result, initially a strictly positive distribution was assumed. The obtained distribution showed very strong peak at about 2.2 au along $\langle 100\rangle$ direction. Similar peaks along $\langle 110\rangle$ and $\langle 111\rangle$ directions did not exceed 20% of the $\langle 100\rangle$ peak height. The peak along (and in the vicinity of) the $\langle 100\rangle$ direction also showed some splitting. All of these features did not seem to be physical and the conclusion was that one has to use a two-channel MEM. For $\alpha = 0.1$ or

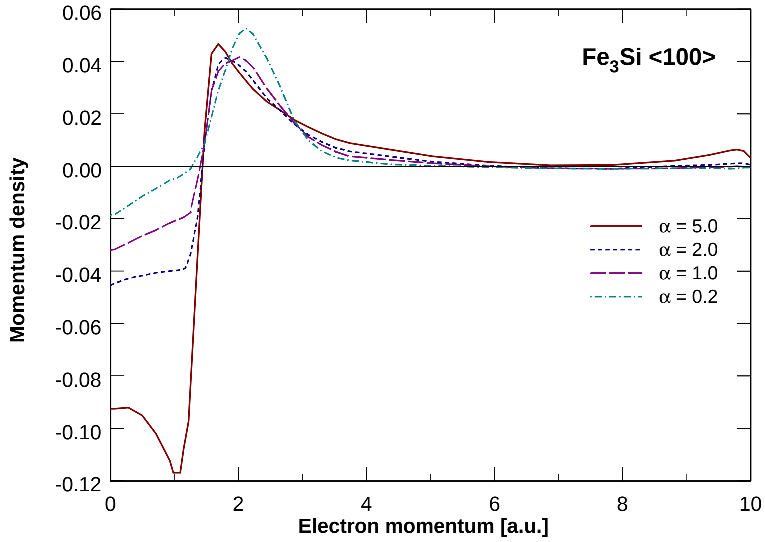

Figure 6. Fe_3Si: the distributions of the momentum density of the electrons with uncompensated spins along the $\langle 100 \rangle$ direction for different choices of the parameter α.

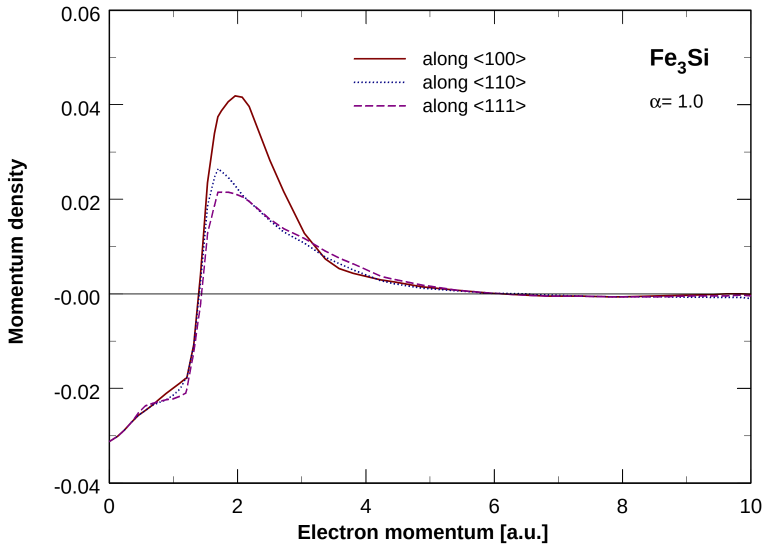

Figure 7. The distributions obtained for high-symmetry directions in Fe_3Si when $\alpha = 1$.

0.2 one obtains apparent negative density at high momenta. Moreover, the asphericity of the positive part still seems very exaggerated, see figure 7. With increasing α the asphericity is diminishing and the negative density at large momenta is gradually disappearing. In contrast, at $\alpha = 5$ one obtains relatively high values of the positive densities at high momenta. Therefore based on common sense we would expect that the results obtained for α between 0.5 and 1.0 are the closest to reality. There are apparent differences in the positive momentum densities as compared to the case of iron (see figure 4). These densities integrate to 5.71 μ_B, while the

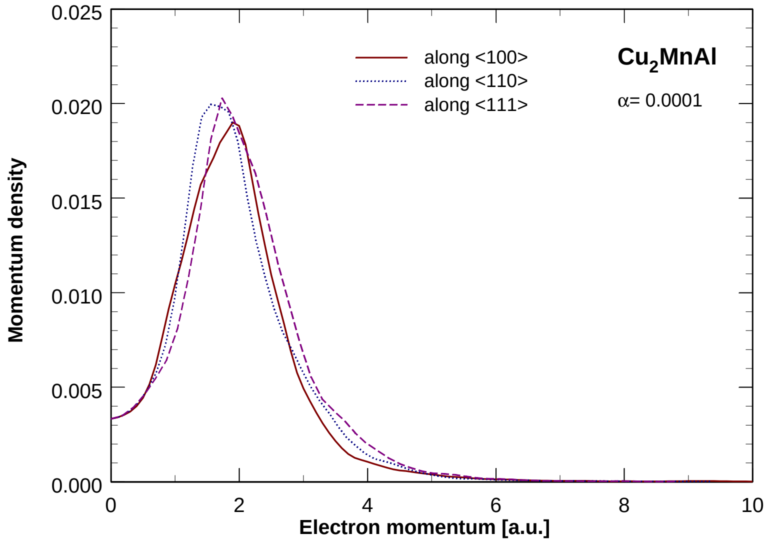

Figure 8. The momentum densities in Cu_2MnAl for the strictly positive case.

negative densities integrate to $-0.75\ \mu_B$. The corresponding values obtained for $\alpha = 0.5$ are about 5.46 and $-0.50\ \mu_B$, so we see that the negative moment turns out to be quite substantial anyway, of the order of $-(0.12\text{–}0.18)\ \mu_B$/atom, i.e. in fact, stronger than in iron.

It is hard to say why the apparent negative moment observed in the Compton scattering does not show up in the neutron case. It seems that it would be worthwhile to repeat the neutron measurements for a different sample than the one used in the original experiment by Moss and Brown (1972). A substantial correction for the extinction, which had to be used in the cited experiment, could result in such an accidental lowering of the form-factor values at the most intense reflections that the negative magnetization densities did not appear in the analysis of the neutron data.

6. Momentum density distribution for electrons with uncompensated spins in Cu_2MnAl

The magnetic Compton scattering on Heusler alloy, Cu_2MnAl, was studied recently by Zukowski *et al* (1997). The main objective of these studies was to check whether the conduction band is positively polarized, as could follow from the neutron diffraction experiment. As was shown, the magnetic Compton profiles exhibited typical crater-like structure, which could be interpreted as showing the negative polarization of the conduction band. The first feature which appeared was that the density obtained in the low momentum region was always very small. In fact, one could easily reconstruct the searched for density without invoking any negative part. Such a strictly positive reconstruction is presented in figure 8. The distribution is almost spherically symmetric, which is expected based on both neutron and Compton scattering results while the density at zero is positive. Of course, this indicates that the conduction electron polarization may indeed be positive. If one believes that the main reason to have a crater around $p = 0$ au is the presence of the negative polarization of the conduction band, the result shown in figure 8 only says that this polarization does not off-set the positive magnetization of the d electrons. However, in light of our discussion at the end of section 4, it seems that the earlier interpretation of the magnetic Compton profiles (Zukowski *et al* 1997) as showing negative polarization of the conduction band could be not well grounded.

7. Conclusions

The paper shows that the two-channel maximum entropy method can be successfully applied to the reconstruction of the momentum density for electrons with uncompensated spins when some physical information about this density distribution is available. One can also hope that once a good prior is chosen a single-channel MEM can be used as well.

We have investigated the three-dimensional electron momentum density distribution for electrons with uncompensated spins in iron, Fe_3Si and in the Heusler alloy, Cu_2MnAl. Whereas the results for Fe and Fe_3Si look very similar, the analysis of the data for the latter alloy could be performed under an assumption of a strictly positive distribution.

The very first conclusion which can be drawn from these facts is that the negative polarization of the conduction band in iron and in Fe_3Si are of similar magnitude, while the one in Cu_2MnAl must be much smaller, if exists at all, which explains why it was not seen in the neutron experiment.

However, a closer look at the values of negative magnetic moments obtained in the course of analysis for iron and Fe_3Si makes us suspicious whether the crater-like structure is entirely due to the conduction band. If this was so, the polarization of this band would be much higher than the theoretical predictions show. Therefore we are inclined to think that the craters are also natural for the d-part of the densities and can appear e.g. as a consequence of the exchange polarization among d electrons. It is known that such an effect contracts wavefunctions of electrons with up spins and pushes wavefunctions of the other electrons away from the atomic centre. Therefore a negative d-type moment should appear far away from the atom, which means that such a moment could appear in the vicinity of $p = 0$ au. Our strictly experimental observation recently found important support in the theoretical analysis of the magnetic Compton profile of nickel (Dixon *et al* 1998), where indeed it has been found that one of the d bands gives a strong negative contribution to the magnetic Compton profile at small momenta. It seems that now we can better understand results of the magnetic neutron diffraction and the magnetic Compton scattering experiments.

Acknowledgments

The work was sponsored by the Polish Committee of Scientific Research through grant No 2 P03B 061 08. Special thanks are due to Professor Andrzej Holas for many useful discussions and invaluable help in numerical analysis.

References

Dixon M A G, Duffy J A, Gardelis S, McCarthy J E, Cooper M J, Dugdale S B, Jarlborg T and Timms D N 1998 *J. Phys.: Condens. Matter* **10** 2759

Dobrzynski L 1974 *INR Report* 1493/II/PS

——1995 *J. Phys.: Condens. Matter* **7** 1373

Dobrzynski L and Holas A 1995 *Informal Proc. 2nd Int. Workshop on Compton Scattering and Fermiology (Tokyo, 1995)* ed N Shiotani, pp 205–14

——1996 *Nucl. Instrum. Methods* A **383** 589

Dobrzynski L, Papoular R and Sakata M 1996 *J. Phys. Soc. Japan* **1** 255

Erickson G J and Smith C R (eds) 1988 *Maximum Entropy and Bayesian Methods in Science and Engineering* vols 1 and 2 (Dordrecht: Kluwer)

Eriksson O, Boring A M, Albers R C, Fernando G W and Cooper B R 1992 *Phys. Rev.* B **45** 2868

Gull S F and Skilling J 1989 *MemSys3 (Quantified Maximum Entropy Subroutine Library)* (Meldreth, UK: Maximum Entropy Data Consultants Ltd)

Jauch W 1994 *Acta Crystallogr.* A **50** 650

Jaynes E T 1983 *Papers on Probability, Statistics and Statistical Physics* ed R D Rosenkrantz (Dordrecht: Kluwer)
Mohammad-Djafari A and Demoment G (eds) 1993 *Maximum Entropy and Bayesian Methods* (Dordrecht: Kluwer)
Moss J and Brown P J 1972 *J. Phys. F: Met. Phys.* **2** 358
Papoular R and Gillon B 1990 *Europhys. Lett.* **13** 429
Sakata M and Sato M 1990 *Acta Crystallogr.* A **46** 263
Sakata M, Uno T, Takata M and Howard C J 1993 *J. Appl. Crystallogr.* **26** 159
Shull C G and Yamada Y 1962 *J. Phys. Soc. Japan* **17** (Supplement B-III) 1
Skilling J (ed) 1988 *Maximum Entropy and Bayesian Methods* (Dordrecht: Kluwer)
——1989 *Maximum Entropy and Bayesian Methods* (Dordrecht: Kluwer)
Smith C R and Grandy W T Jr (eds) 1985 *Maximum Entropy and Bayesian Methods in Inverse Problems* (Dordrecht: Kluwer)
Tanaka Y, Sakai N, Kubo Y and Kawata H 1993 *Phys. Rev. Lett.* **70** 1537
van Laar B, Maniawski F, Kaprzyk S and Dobrzynski L 1980 *Nukleonika* **25** 835
Zukowski E, Andrejczuk A, Dobrzynski L, Cooper M J, Dixon M A G, Gordelis S, Lawson P K, Buslaps T, Neumann K-U and Ziebeck K R A 1997 *J. Phys.: Condens. Matter* **9** 10 993
Zukowski E, Andrejczuk A, Dobrzynski L, Kaprzyk S, Cooper M J, Duffy J and Suortti P 2000, to be published